GLYCOBIOLOGY AND EXTRACELLULAR MATRICES:

Candida albicans Phospholipomannan, a New Member of the Fungal Mannose Inositol Phosphoceramide Family

Pierre-André Trinel, Emmanuel Maes, Jean-Pierre Zanetta, Florence Delplace, Bernadette Coddeville, Thierry Jouault, Gérard Strecker and Daniel Poulain

J. Biol. Chem. 2002, 277:37260-37271.
doi: 10.1074/jbc.M202295200 originally published online July 22, 2002

THE JOURNAL OF BIOLOGICAL CHEMISTRY
Vol. 277, No. 40, Issue of October 4, pp. 37260–37271, 2002

Printed in U.S.A.

Candida albicans Phospholipomannan, a New Member of the Fungal Mannose Inositol Phosphoceramide Family*

Received for publication, March 8, 2002, and in revised form, July 22, 2002
Published, JBC Papers in Press, July 22, 2002, DOI 10.1074/jbc.M202295200

Pierre-André Trinel‡, Emmanuel Maes§, Jean-Pierre Zanetta§, Florence Delplace§, Bernadette Coddeville§, Thierry Jouault‡, Gérard Strecker§, and Daniel Poulain‡¶

From the ‡Laboratoire de Mycologie Fondamentale et Appliquée, Inserm EPI 9915, Faculté de Médecine, Pôle Recherche, 59037, Lille Cedex, France, and §Laboratoire de Glycobiologie Structurale et Fonctionnelle, CNRS Unité Mixté de Recherche No. 8576, Laboratoire de Chimie Biologique, Université des Sciences et Technologies de Lille, 59655 Villeneuve d'Ascq, France

The pathogenic yeast *Candida albicans* has the ability to synthesize unique sequences of β-1,2-oligomannosides that act as adhesins, induce cytokine production, and generate protective antibodies. Depending on the growth conditions, β-1,2-oligomannosides are associated with different carrier molecules in the cell wall. Structural evidence has been obtained for the presence of these residues in the polysaccharide moiety of the glycolipid, phospholipomannan (PLM). In this study, the refinement of purification techniques led to large quantities of PLM being extracted from *Candida albicans* cells. A combination of methanolysis, gas chromatography, mass spectrometry, and nuclear magnetic resonance analyses allowed the complete structure of PLM to be deduced. The lipid moiety was shown to consist of a phytoceramide associating a C_{18}/C_{20} phytosphingosine and C_{25}, C_{26}, or mainly C_{24} hydroxy fatty acids. The spacer linking the glycan part was identified as a unique structure: -Man-P-Man-Ins-P-. Therefore, in contrast to the major class of membranous glycosphingolipids represented by mannose diinositol phosphoceramide, which is derived from mannose inositol phosphoceramide by the addition of inositol phosphate, PLM seems to be derived from mannose inositol phosphoceramide by the addition of mannose phosphate. In relation to a previous study of the glycan part of the molecule, the assignment of the second phosphorus position leads to the definition of PLM β-1,2-oligomannosides as unbranched linear structures that may reach up to 19 residues in length. Therefore, PLM appears to be a new type of glycosphingolipid, which is glycosylated extensively through a unique spacer. The conferred hydrophilic properties allow PLM to diffuse into the cell wall in which together with mannan it presents *C. albicans* β-1,2-oligomannosides to host cells.

Sphingolipids are ubiquitous and essential components of living cells found mainly on the outer leaflet of plasma membranes (1–3). Along with their role in membrane permeability and fluidity, they have also been shown to act as second messengers produced in response to various stress situations, which regulate basic processes such as cell cycle control, apoptosis (4), cell-cell interactions (1), and immune response (5).

Sphingolipids are ceramide structures composed of a long chain base whose amino group is amide-linked to various fatty acids. This basic structure as well as those derived by the addition of polar groups such as phosphocholine or carbohydrates to the ceramide may vary according to the species (6–8). It has been established that sphingolipids from fungal and mammalian cells display important differences in their fine structure and biosynthetic pathways (9). Fungal species incorporate phytosphingosine (PHS)[1] and presumably dihydrosphingosine in the ceramide moieties instead of the sphingosine used mainly by mammals and also have longer fatty acids (C_{24}-C_{26} instead of C_{16}-C_{18}) (9). Fungi then preferentially add inositol to the ceramide group, leading to the family of inositol phosphoceramides composed of inositol phosphoceramide (IPC), mannose inositol phosphoceramide (MIPC), and mannose diinositol phosphoceramide ($M(IP)_2C$) instead of phosphocholine in mammalian cells (9). These differences between mammalian cells and fungi represent a target for antifungal drugs such as aureobasidin A (10) and khafrefungin (11), which inhibit IPC synthase. Along with sphingomyelin of mammals and IPCs of fungi and plants, glycosylceramides are another important class of sphingolipids described in fungi and mammals in which the sugar moiety is directly linked to the ceramide (6). The biosynthetic pathway of fungal sphingolipids has only been studied in the yeast *Saccharomyces cerevisiae*. Numerous steps in the pathway are still unknown (12), and the enzymes involved have not yet been purified or characterized. This lack of knowledge contrasts with the key role of these molecules in cell growth (13) and viability (10), resistance to various environmental stresses (14), remodeling of glycosyl phosphatidylinositol anchors (15), endocytosis (16), and calcium homeostasis (17).

Although *Candida albicans* is the prominent opportunistic fungal pathogen causing mucocutaneous and systemic infections (18, 19), almost nothing is known about its sphingolipids with the exception that a glucosylceramide has been described

* This work was supported by the "Réseau Infection Fongique" du Ministère Français de l'Education Nationale de la Recherche et de la Technologie (MNERT). The costs of publication of this article were defrayed in part by the payment of page charges. This article must therefore be hereby marked "*advertisement*" in accordance with 18 U.S.C. Section 1734 solely to indicate this fact.

¶ To whom correspondence should be addressed. Tel.: 33-3-20-62-34-20; Fax: 33-3-20-62-34-16; E-mail: dan_poulain@compuserve.com.

[1] The abbreviations used are: PHS and **SP**, phytosphingosine; IPC, inositol phosphoceramide; MIPC, mannose inositol phosphoceramide; $M(IP)_2C$, mannose diinositol phosphoceramide; PLM, phospholipomannan; GC, gas chromatography; MS, mass spectrometry; **IN** and Ins, inositol; Man, mannose; HMQC, homonuclear multiple quantum correlation spectroscopy; ROESY, Rotating frame nuclear Overhauser enhancement spectroscopy; FA, fatty acid; rC_{20} PHS, PHS with 20 carbons chain ramified at the position $\omega(n\text{-}3)$; OH rC_{24} FA, hydroxylated FA with 24 carbons chain ramified at the position $\omega(n\text{-}3)$; rC_{20} PHS-OH rC_{24} FA, ceramide structure composed of rC_{20} PHS linked to a OH rC_{24} FA.

previously (20) and that IPCs, MIPC, and $M(IP)_2C$ have recently been characterized in its hyphal form (21). In a series of studies, some immunochemical properties of a *C. albicans* glycolipid containing long chains of β-1,2-linked mannose residues have been demonstrated and characterized previously (22). *C. albicans* β-1,2-oligomannosides, which act as adhesins (23, 24), induce cytokine production, and generate protective antibodies (25, 26), are considered to be among the virulence factors of this species. Using a model of *C. albicans* macrophage interaction, it was shown that phospholipomannan (PLM) shed by *C. albicans* acted as a vector for β-1,2-oligomannosides in inducing strong cellular stimulation (27).

The aim of this study was to investigate the complete structure of this pathophysiologically relevant molecule of *C. albicans.* A purification procedure was developed to obtain large quantities of soluble PLM, and phase gas chromatography (GC) coupled to mass spectrometry (MS) analysis of methanolysis products, extensive NMR, and MS analyses were carried out. A combination of the results of these analyses allowed the complete structure of PLM to be determined and demonstrated that PLM is a new type of mannose inositol phosphoceramide.

EXPERIMENTAL PROCEDURES

Strain and Growth Conditions—*C. albicans* serotype A, strain VW32, was used throughout this study. For large scale cell production, cells were preincubated on Sabouraud's agar for 18 h at 28 or 37 °C and then inoculated at a concentration of 10^6 cells/ml in 1-liter Erlenmeyer flasks containing 500 ml of Sabouraud's broth. Growth was performed to stationary phase at 28 or 37 °C on an orbital shaker (180 rpm). Cells were finally collected by centrifugation.

Purification of PLM—Cells were broken with a French press (Aminco) at 20,000 p.s.i, dialyzed, and lyophilized. PLM was then extracted and purified as described previously (22) with the exception that care was taken to avoid micelle formation to improve PLM solubility for NMR studies. Modifications to the method were mainly the lyophilization of most water phases or fractions instead of centrifuge concentration and the reduced use of highly concentrated water phases. The main steps in PLM purification were as follows: (i) extraction with various chloroform/methanol and chloroform/methanol/water mixtures; (ii) extensive butanol/water partitions; and (iii) hydrophobic interaction on phenyl-Sepharose using increasing concentrations of ethanol (1–40%) for elution. Purification and control of PLM fractions were followed by thin-layer chromatography (TLC) (22) and Western blot analysis using the mouse IgM monoclonal antibody, DF9-3 (28).

Monosaccharide and Lipid Composition of PLM—Samples (1–5 μg) of purified PLM were lyophilized in conical heavy walled Pyrex tubes (2.0 ml) with Teflon lined screw caps. Methanolysis reagent (0.25–0.5 ml) was then added, and the closed vessels were left for 20 h at 80 °C. The methanolysis reagent was obtained by dissolving anhydrous gaseous HCl (up to 0.5 M) at −50 °C in anhydrous methanol previously redistilled on magnesium turnings (29). Gaseous HCl was prepared by the dropwise addition of concentrated sulfuric acid onto crystallized sodium chloride. After methanolysis, samples were evaporated to dryness under a light stream of nitrogen in a ventilated hood followed by the addition of 200 μl of acetonitrile and 25 μl of heptafluorobutyric anhydride with a pipette with plastic tips. The closed vessels were heated for 15 min at 150 °C in a sand bath. After cooling to room temperature, the samples were evaporated in a light stream of nitrogen in a ventilated hood to eliminate excess reagent, and samples were then submitted to a further methanolysis followed by acylation with heptafluorobutyric anhydride as described above. This second methanolysis and acylation step was found necessary for complete cleavage of phosphodiester bonds (and when present, of the linkage between glucosamine and inositol which is observed in glycosylphosphatidylinositols). After drying, the sample was taken up in 200 μl of acetonitrile previously dried on calcinated calcium chloride, and an aliquot was introduced into the Ross injector of the GC apparatus.

GC/MS Analysis—For GC/MS analysis, the GC separation was performed on a Carlo Erba GC 8000 gas chromatograph equipped with a 25-m × 0.32-mm CP-Sil5 CB Low Bleed/MS capillary column 0.25-μm film phase (Chrompack France, Les Ullis, France). The temperature of the Ross injector was 260 °C, and the samples were analyzed using the following temperature program: 90 °C for 3 min and then 5 °C/min until reaching 240 °C. The column was coupled to a Finnigan Automass II mass spectrometer. The analyses were performed in the electron impact mode (ionization energy 70 eV, source temperature 150 °C). As described previously (29–31), this method allowed the identification and the quantification of all constituents of glycolipids in a single GC/MS analysis.

Mass Spectrometry—Electrospray mass measurements were carried out in negative ion mode on a triple quadrupole instrument (Micromass Ltd, Altrincham, United Kingdom) fitted with an atmospheric pressure ionization electrospray source. A mixture of polypropylene glycol was used to calibrate the quadrupole mass spectrometer. The samples were dissolved in dimethyl sulfoxide and further diluted in methanol to obtain a final concentration of ~1 μg/μl. Solutions were infused using a Harvard syringe pump at a flow rate of 3 μl/min. The quadrupole was scanned from 600 to 2200 Da with a scan duration of 5 s and a scan delay of 0.1 s. The samples were sprayed using a 3.5-kV needle voltage, and the declustering cone was set at 70 V.

NMR Experiments—Samples (PLM-28 and PLM-37) were repeatedly treated with ^2H_2O (99.97% ^2H atoms, Euriso-top, CEA, Saclay, France) and then dissolved in 250 μl of Me_2SO-d_6 (99.98% ^2H, Euriso-top). ^1H and ^{13}C chemical shifts were expressed in parts/million downfield from the signal of Me_2SO-d_6 methyl group (δ^1H = 2.50 and $\delta^{13}C$ = 40.55 ppm), and ^{31}P chemical shifts were referenced to external H_3PO_4 (δ = 0.00 ppm). Samples were analyzed in 200 × 5-mm BMS-005B Shigemi® tubes at 343 K on a Bruker® ASX-400 spectrometer (^1H = 400.33, ^{13}C = 100.66, and ^{31}P = 162.5 MHz) equipped with a double resonance ($^1H/X$) broadband inverse z-gradient probe head. All NMR samples were recorded without sample spinning.

The one-dimensional proton ^1H spectra were measured using a 90° tipping angle for the pulse and 1.5 s as a recycle delay between each 32 acquisitions of 2.4 s. The spectral width of 4006 Hz was collected in 16,000 complex data points. One-dimensional ^{13}C was recorded using a spectral width of 20,161 Hz, and 32,768 data points were collected to obtain a field induction decay resolution of 0.6 Hz/point. The ^{31}P spectra of both compounds were acquired with a spectral width of 16,233 Hz collected in 16,384 data points. Both experiments were carried out with composite pulse decoupling during acquisition using globally optimized alternating phase rectangular pulse sequence at the carbon or phosphorus frequency. An exponential transformation (line broadening factor = 6 Hz for ^{13}C and 4 Hz for ^{31}P) was applied prior to processing data points in the frequency domain. Two-dimensional homonuclear (^1H-^1H) COSY, one-step relayed COSY, two-step relayed COSY and ROESY, and heteronuclear ^1H-^{13}C HMQC, ^1H-^{31}P HMQC, and HMQC-HOHAHA spectroscopy were carried out using standard Bruker pulse programs (cosy, cosyrl, cosyr2, roesytp, inv4tp, inv4mlevtp, respectively). All of the experiments were carried out in the time-phase proportional increment with the exception of COSYs, which were conducted in a magnitude mode. Finally, two-dimensional HMQC-HOHAHA spectroscopy was recorded using Malcom Lewitt-17 mixing sequences with a mixing time of 120 ms for both ^{13}C and ^{31}P nuclei. Two-dimensional ROESY spectra were obtained with mixing times of 400 ms. All of the parameters including special delays were carried out in each experiment.

RESULTS

Analysis of Molar Composition of PLM Revealed That the β-Oligomannoside Chain Is Anchored to a Ceramide Moiety—Our GC/MS analysis of the methanolysis products of PLM allowed us to establish in a single experiment the identification and respective ratio of each PLM component (Table I). It revealed for PLMs synthesized by *C. albicans* strain VW32 at 28 °C (PLM-28) or 37 °C (PLM-37) an average composition of 12 or 13 mannose residues for one inositol, one long chain base and one fatty acid. The major long chain bases were identified by their electron impact spectra (Fig. 1) as the 1,3,4-trihydroxy-2-amino-15-methyl-heptadecane (ramified C_{18} phytosphingosine or rC_{18} PHS) (Fig. 1*c*) and 1,3,4-trihydroxy-2-amino-15-methyl-nonadecane (rC_{20} PHS) (Fig. 1*d*). Minor components were identified as 1,3,4-trihydroxy-2-amino-octadecane and 1,3,4-trihydroxy-2-amino-eicosane (Fig. 1*e*), *i.e.* the corresponding non-ramified PHSs. The major fatty acid (FA) was 2-hydroxy-21-methyl-tricosanoate, a ramified hydroxylated fatty acid with 24 carbon atoms (OH rC_{24} FA) (Fig. 1*b*). Other fatty acids were the homologues with 25 and 26 carbon atoms all

TABLE I

Comparison of the composition of phospholipomannans synthesized by C. albicans VW32 at 28 and 37 °C

Samples were submitted to two consecutive runs of methanolysis/HFBAA acylation and then analyzed by GC-MS. LCB, long chain bases.

	Molar composition		FA		LCB	
	Component	No. residues	Component	Total FA	Component	Total LCB
				%		%
Phospholipomannan (28 °C)	Mannose	12.07	OH rC_{24}[c]	71.16	rC_{18} PHS[c]	52.81
	Inositol	0.987	OH rC_{25}	4.75	C_{18} PHS	2.68
	Fatty acid[a]	0.992	OH rC_{26}	6.22	rC_{20} PHS	41.8
	LCB[b]	1.00	$C_{16:0}$	7.63	C_{20} PHS	2.69
			$C_{18:0}$	7.96		
			$C_{18:1}$	2.28		
Phospholipomannan (37 °C)	Mannose	13.21	OH rC_{24}	70.21	rC_{18} PHS	29.13
	Inositol	0.891	OH rC_{25}	9.02	C_{18} PHS	2.19
	Fatty acid[a]	0.975	OH rC_{26}	4.54	rC_{20} PHS	64.54
	LCB[b]	1.00	$C_{16:0}$	9.68	C_{20} PHS	4.12
			$C_{18:0}$	6.53		

[a] See the details of the fatty acids composition in the column Fatty Acids.
[b] See the details of the long chain base composition in the column Long Chain Base.
[c] r refers to a ramification of the chain in the position $\omega(n-3)$.

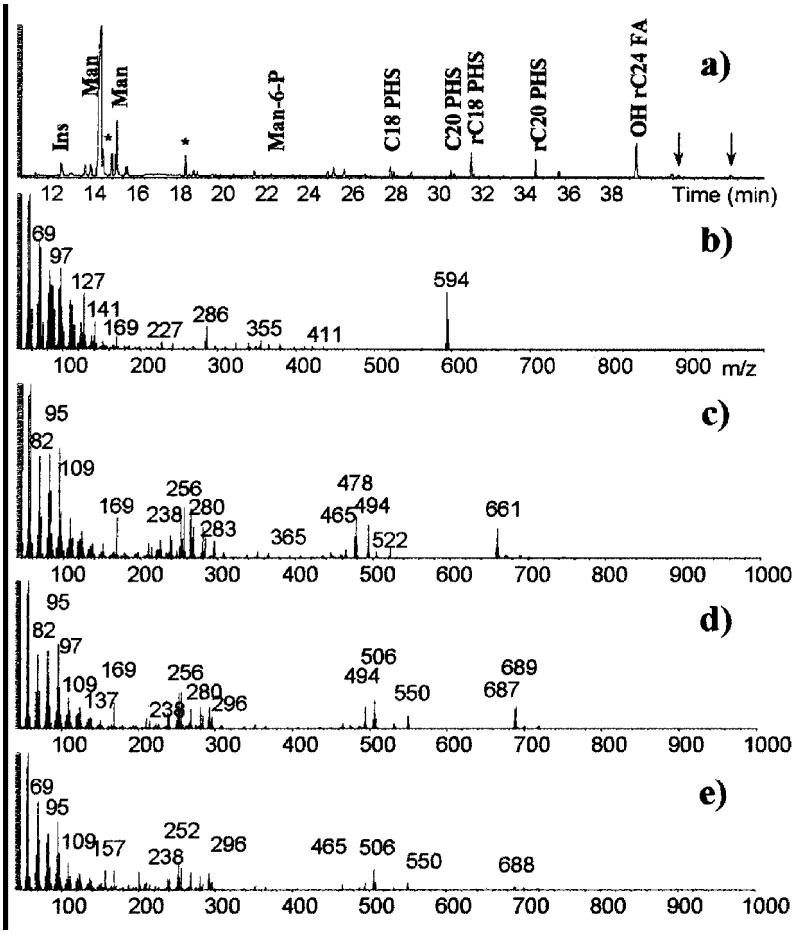

FIG. 1. **GC/MS analysis of methanolysis products from purified PLM-28.** Phospholipomannan was subjected to two consecutive runs of methanolysis and heptafluorobutyric anhydride treatment and analyzed by GC/MS in the electron impact mode of ionization. *a*, total ion count profile. rC_{18} PHS and rC_{20} PHS refer to ramified phytosphingosines with a chain length of 18 and 20 carbon atoms, respectively. The major peaks corresponded to the furanic forms produced by dehydration between carbons 1 and 4 during anhydrous acid-catalyzed methanolysis. OH rC_{24} FA represents 2-hydroxy-21-methyl-tricosanoate. The *arrows* indicate the presence of homologous compounds with one and two additional carbon atoms. *, unidentified compound. *b–e*, mass spectra in the electron impact mode. *b*, 2-hydroxy-21-methyl-tricosanoate: 594 = $[M^+\cdot]$. The ions at *m/z* 286 and 355 are characteristic of 2-OH fatty acids methyl esters (30) (*b*), furanic form of 1,3,4-trihydroxy-2-amino-15-methyl-heptadecane (*c*), 1,3,4-trihydroxy-2-amino-15-methyl-nonadecane (*c*). For *c* and *d*, the ions at 252, 256, and 494 are characteristic of the furanic form of phytosphingosines. The ions at *m/z* 661 and 689 ($[M-30]^+$) are because of the loss of CH_2=O. *e*, 1,3,4-trihydroxy-2-amino-eicosane. For the details of fragmentation patterns, see study by Pons *et al.* (30).

hydroxylated on carbon 2 and ramified in the $\omega(n\text{-}3)$ position (OH rC_{25} FA and OH rC_{26} FA, respectively). Linear fatty acids (hexadecanoate and octadecanoate) were also present at a lower level. No trace of monosaccharides other than mannose was detected. In contrast, a small peak with a typical fragmentation pattern revealed the presence of mannose-6-phosphate.

The molar composition of PLM-28 and PLM-37 appeared to be similar as did their OH rC_{24} FA ratio (Table I). The main modifications concerned an inversion of the relative ratios of OH rC_{25} FA and OH rC_{26} FA and a marked inversion of rC_{18} PHS and rC_{20} PHS, the latter becoming the most abundant in PLM-37.

MS Analysis of PLM Revealed Crossed Heterogeneity Arising from Its Carbohydrate and Lipid Moieties—Electrospray mass spectra of PLM-37 (Fig. 2*a*) and PLM-28 (Fig. 2*b*) demonstrated a series of groups of five peaks that covered the entire spectra. Among these groups, those spaced by an average *m/z* ratio of 81 were observed. These corresponded to (M − 2H)/2 molecular-related ions and consequently to the varying degrees of polymerization of the glycan chain of PLM seen in a previous study (22). Conversely, the five peaks within each group arose from heterogeneity of the lipid part of PLM, because they displayed spaced *m/z* ratios of 7, which therefore corresponded to a mass change of 14 (one CH_2 group). According to the results of

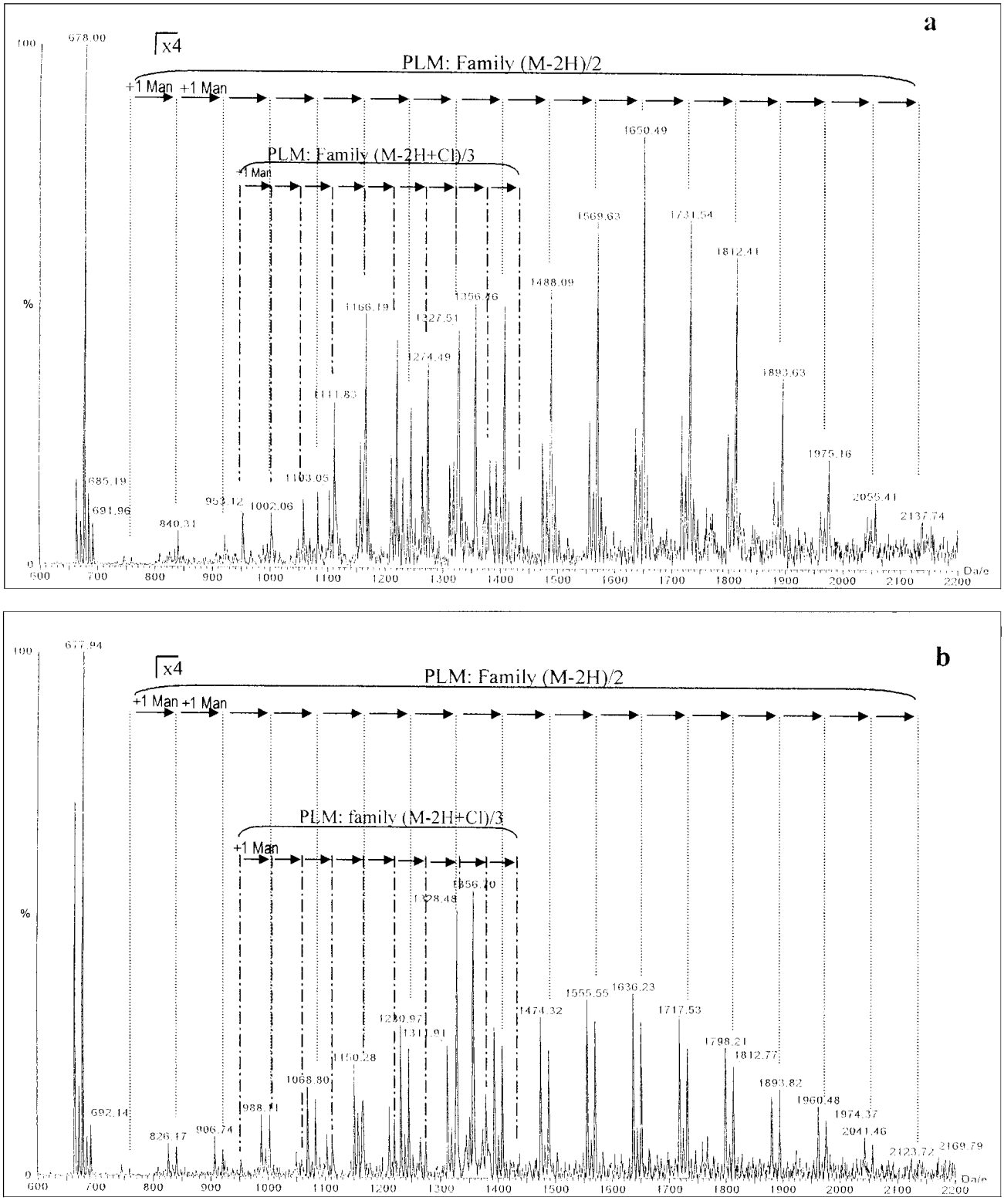

FIG. 2. **Electrospray mass spectra of phospholipomannan synthesized by *C. albicans* strain VW32 at 37 (*a*) and 28 °C (*b*).** Two complex families of molecular-related ions, (M − 2H)/2 (for example, *m/z* 1650.49) and (M − 2H + Cl)/3 (for example, *m/z* 1274.49), that partially overlapped were produced from the original molecules. For each family, groups of peaks corresponded to the various degrees of polymerization of the glycan part, and peaks within each group arose from the variability of the lipid part. The shift observed for the main peak of each group between PLM-37 and PLM-28 corresponds to a change of the number of carbons of the phytosphingosine unit. The *m/z* values observed on these spectra differed slightly from the values reported in Table II because of smoothing of the spectra.

GC/MS analysis of methanolysis products and to the relative ratios of their lipid components, these peaks can be attributed to the different compositions of the ceramide moiety as shown in Table II for PLM-37. This interpretation of the results was confirmed when the PLM-28 and PLM-37 spectra were compared (Figs. 2, *a* and *b*), because at 28 °C, for each degree of

TABLE II
Negative ion ES-mass spectrometry of PLM-37
Examples of the masses and molar ratios deduced from chosen groups in each family of molecular-related ions detected

Average measured	Molecular-related ion	Deduced average mass value	Composition (number of residues)[a]					Mass increment in the same family
			Man	Ins	PHS	FA	PO3H	
m/z								
1636.68	(M − 2H)/2	3275.37	14	1	1 rC_{18}	1 OH rC_{24}	2	
1644.04	(M − 2H)/2	3290.09	14	1	1 rC_{18}	1 OH rC_{25}	2	
1650.63	(M − 2H)/2	3303.27 (Major)[b]	14	1	1 rC_{20}	1 OH rC_{24}	2	+ 161.93
		3303.27 (Minor)[b]	14	1	1 rC_{18}	1 OH rC_{26}	2	
1657.80	(M − 2H)/2	3317.61	14	1	1 rC_{20}	1 OH rC_{25}	2	
1665.01	(M − 2H)/2	3332.03	14	1	1 rC_{20}	1 OH rC_{26}	2	
1731.59	(M − 2H)/2	3465.19 (Major)[b]	15	1	1 rC_{20}	1 OH rC_{24}	2	
		3465.19 (Minor)[b]	15	1	1 rC_{18}	1 OH rC_{26}	2	
1210.62	(M − 2H + Cl)/3	3598.42	16	1	1 rC_{18}	1 OH rC_{24}	2	
1215.89	(M − 2H + Cl)/3	3614.23	16	1	1 rC_{18}	1 OH rC_{25}	2	
1220.38	(M − 2H + Cl)/3	3627.70 (Major)[b]	16	1	1 rC_{20}	1 OH rC_{24}	2	+ 161.91
		3627.70 (Minor)[b]	16	1	1 rC_{18}	1 OH rC_{26}	2	
1224.89	(M − 2H + Cl)/3	3641.23	16	1	1 rC_{20}	1 OH rC_{25}	2	
1274.35	(M − 2H + Cl)/3	3789.61 (Major)[b]	17	1	1 rC_{20}	1 OH rC_{24}	2	
		3789.61 (Minor)[b]	17	1	1 rC_{18}	1 OH rC_{26}	2	

[a] Composition of the molecules was defined according to their mass and the results of methanolysis analysis.
[b] Major and minor refers to the relative contribution of the two components to a same peak.

polymerization of the glycan chain, an inversion of the relative importance of the two main peaks of each group was observed, which arose from changes in the ceramide moiety (*i.e.* rC_{18} PHS − OH rC_{24} FA and rC_{20} PHS − OH rC_{24} FA). This change must be related to the inversion of the relative molar ratios of the long chain bases as revealed by methanolysis. This observation was also confirmed by inversion of the minor peaks corresponding to rC_{20} PHS − OH rC_{25} FA and rC_{20} PHS − OH rC_{26} FA in agreement with methanolysis analysis. A second family of groups of five peaks was also observed mainly in the left part of the spectra (Fig. 2, *a* and *b*), which most probably corresponded to (M − 2H + Cl)/3 molecular-related ions. These groups of peaks were spaced by an average *m/z* ratio of 54 (1 Man/3) and therefore also arose because of the varying degrees of polymerization of the glycan part of PLM (Table II). Peaks within each group were spaced by an average *m/z* ratio of 4.66, which corresponded to a mass variation of 14 arising from the lipid part (Table II). As confirmed from their respective spacing, groups of peaks from the two families regularly overlapped, leading to common groups of peaks, *i.e.* groups with a main peak at *m/z* 1166.19 or 1327.51 on Fig. 2*a*. This finding was also confirmed by a slight shift of the *m/z* values (data not shown) and from a modification of the relative ratios of the peaks within these groups explained by the heterogeneous overlapping of the families, because they vary respectively according to M/3 and M/2.

Therefore, the two families of groups of peaks observed in the two spectra appeared to originate from the same native molecules. According to these results, PLM may contain 3–20 Man residues/molecule with PLM containing 14 Man residues being the most abundant. In both spectra, the two main peaks at *m/z* ~678 and ~1357 appeared unrelated to the PLM families and seemed to correspond to (M − 2H)/2 and (M − H) molecular-related ions from the same molecule, which according to its mass and the results of NMR analysis (see below) is probably $M(IP)_2C$. As observed for PLM, $M(IP)_2C$ is also heterogeneous and seems to express the same variability in its ceramide moiety.

NMR Analysis of PLM Revealed That a Specific Spacer Is Used to Anchor the β-1,2-Man Polymer to the PHS of the Ceramide Moiety—Low solubility of glycolipids leads to micelle formation, which affects the relaxation time of molecules in NMR experiments. Therefore, previous NMR analysis of PLM has been restricted to water-soluble glycans released by alkaline treatment (22). A new PLM preparation procedure, avoiding micelle formation, and the use of Me_2SO-d_6, known to improve the solubility of glycolipids, have allowed NMR studies of the native molecule. In complementation to previous analysis of the glycan part performed in D_2O, this study mainly focused on the structure of the spacer that links glycans (β-1,2-oligomannosides) to the lipid moiety and resolves previous ambiguity regarding the position of the second phosphate group of PLM.

NMR analyses have consisted of: (i) a series of COSY experiments to define the ^1H chemical shifts in the sugar, inositol, fatty acid, and phytosphingosine units; (ii) ^1H-^{13}C and ^1H-^{31}P HMQC correlation experiments to define the ^{13}C chemical shifts and the nature of the phosphodiester bridges; and (iii) a ROESY experiment that has established the linkage anomery of the sugar units, their sequence, and their linkage with inositol and phytosphingosine.

The ^1H NMR spectra of PLM-28 and PLM-37 of *C. albicans* were almost identical, and the anomeric signals of the sugar units were designated **A** to **G** according to the decreasing chemical shift of their resonances (Fig. 3, *a* and *b*). **IN**, **SP,** and **FA** were also used to indicate *myo*-inositol, phytosphingosine, and fatty acid signals, respectively, to avoid excessive spectra overload. Because the coupling constants of the anomeric signals could not be measured accurately, the anomeric configuration of Man units **A** to **G** was established on the basis of their intraresidual connectivities, H-1/H-2 for α-Man and H-1/H-3, H-5 for β-Man by ROESY experiments (see below). The anomeric configuration of α-Man units **A** and **B** was also revealed by their characteristic downfield-shifted ^1H-5 resonance as well as by their upfield-shifted ^{13}C-5 resonance (see Table III). In this way, sugar units **A** and **B** on the one hand and **C** to **G** on the other hand were identified as α- and β-Man units, respectively. Moreover, the relatively high coupling (J_3 = 7.2 Hz), which splits the H-1 resonance of α-Man unit **A**, is most probably attributed to the presence of a phosphate group as confirmed by heteronuclear ^1H-^{31}P NMR spectroscopy.

Because two-dimensional COSY, ROESY, and ^1H-^{13}C or ^1H-^{31}P HMQC spectra of both PLMs were essentially identical (data not shown), the assignment of ^1H and ^{13}C chemical shifts was performed using two-dimensional NMR spectra of PLM-28 or PLM-37.

The starting point for interpretation of the COSY (Fig. 4) and one-step or two-step relayed COSY spectra (data not shown) was the H-1 signal of sugar residues **A** to **G** and the H-5 signal of **IN** and $(CH2)_n$ of **FA** and **SP**. A combination of these NMR analyses allowed the assignment of the ^1H chemical shifts of H-1, H-2, H-3, H-4, H-5, and H-6 of Man units **A** to **G** and also

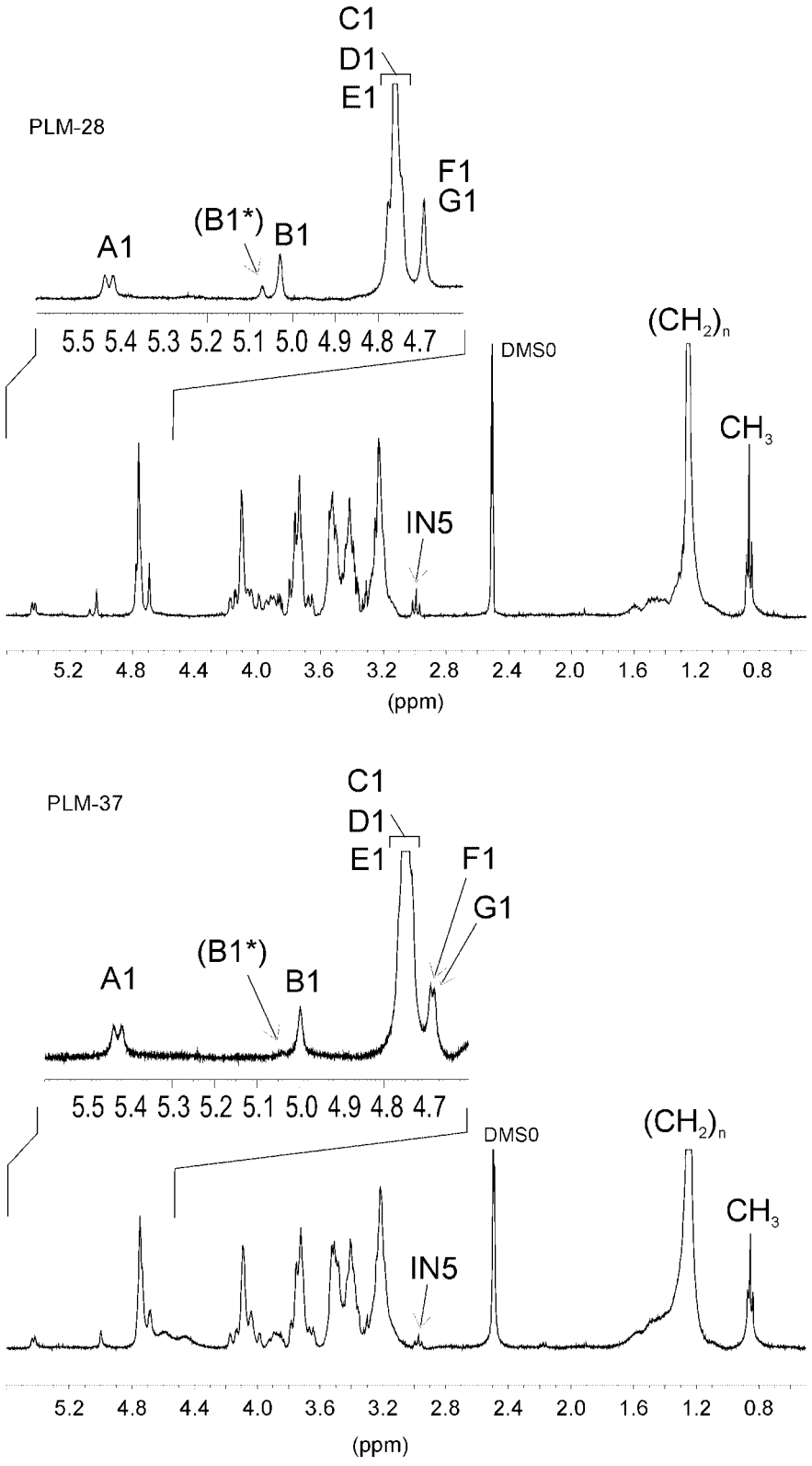

FIG. 3. **^{1}H nuclear magnetic resonance spectra of PLM-28 and PLM-37.** Signals **A** to **G** arose from Man units. **IN** signal arose from inositol, and $(CH_2)_n$ and CH3 signals arose from phytosphingosine and fatty acids.

the assignment of **FA**2, **SP,** and **IN**1–6 resonances (Table III). A split of the **IN**2, **IN**3, and **IN**6 signals (**IN**2*, **IN**3*, and **IN**6*, respectively) was also observed for PLM-28 (Fig. 4) and was attributed to heterogeneity of the material as described below.

The two-dimensional ^{1}H-^{13}C HMQC spectrum of PLM-28 (Fig. 5*a*) allowed the assignment of most of the ^{13}C resonances (Table III) with the exception of those belonging to α-Man unit **B**, which were deduced from a comparison of the ^{1}H-^{1}H COSY, ^{1}H-^{13}C, and ^{1}H-^{31}P HMQC spectra (data not shown). The complete assignment of the ^{13}C resonances was achieved by interpretation of the ^{1}H-^{13}C HMQC-HOHAHA spectrum (Fig. 5*b*). This experiment provided individual C-2 to C-6 resonances of sugar units **G**, **C**, **D**, **A**, **F**, and **E**, starting from their respective H-2 atom resonance as explained in Fig. 5. The complete series of ^{1}H and ^{13}C resonances of the inositol unit was also observed, and the **IN** C-4 and C-6 resonances in particular were clearly

TABLE III
^1H and ^{13}C chemical shifts of structural reporter groups of the PLM-37 isolated from Candida albicans strain VW32, serotype A

Units		Chemical shifts							
		1	2	3	4	5	6	$(CH_2)_n$	CH_3
A	^1H	5.43	4.026	3.647	3.37	3.535	3.65a 3.53b	–	–
	^{13}C	95.38	**79.77**[a]	70.63	69.4	75.47	62.57	–	–
B	^1H	4.999	3.712	3.54	3.53	3.937	3.88a,b	–	–
	^{13}C	102.39	71.85	71.86	67.98	73.67	**65.85**	–	–
C	^1H	4.75	4.127	3.351	3.3	3.20	3.72a 3.50b	–	–
	^{13}C	102.6	**78.52**	73.9	69.24	78.6	62.99	–	–
D	^1H	4.75	4.083	3.46	3.22	3.20	3.72a 3.50b	–	–
	^{13}C	102.6	**81.34**	73.55	69.62	78.22	62.57	–	–
E	^1H	4.751	3.781	3.288	3.368	3.22	3.72a 3.50b	–	–
	^{13}C	102.6	71.2	75.01	68.86	78.24	63.13	–	–
F	^1H	4.692	3.976	3.42	3.25	3.167	3.72a 3.50b	–	–
	^{13}C	100.22	**81.99**	73.5	69.4	78.2	62.57	–	–
G	^1H	4.683	4.16	3.391	3.231	3.124	3.72a 3.50b	–	–
	^{13}C	102.44	**80.99**	73.55	69.5	78.6	62.77	–	–
IN	^1H	3.757	4.045	3.202	3.378	2.975	3.502	–	–
	^{13}C	**76.85**	**79.77**	72.2	73.64	76.81	73.64	–	–
SP	^1H	4.035a 3.755b	3.889	3.45	3.384	–	–	1.24	0.86
	^{13}C	**65.49**	51.82	74.65	72.15	–	–	30.4	15.0
FA	^1H	–	3.845	–	–	–	–	1.24	0.86
	^{13}C	–	72.58	–	–	–	–	30.43	15.02

[a] Boldface numbers refer to downfield shifted ^{13}C resonances arising from a glycosylated or phosphorylated position.

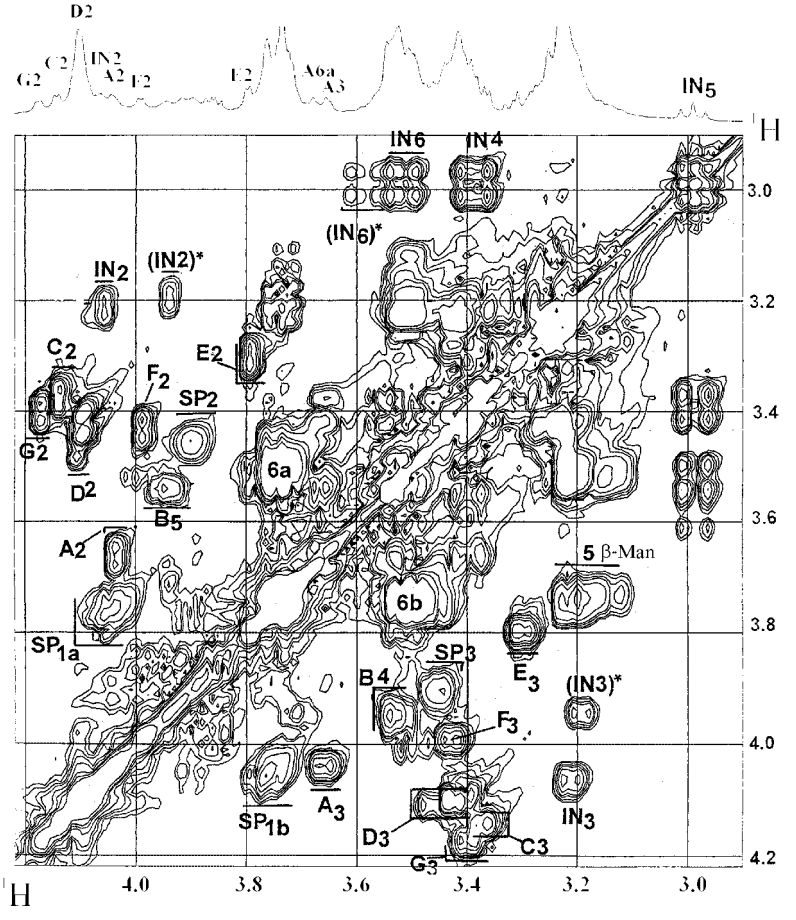

FIG. 4. **COSY spectrum of PLM-28 showing the ^1H chemical shifts of Man units A to G, of SP and of IN**. (**IN**2)*, (**IN**3)*, and (**IN**6)* signals belong to a non-substituted inositol unit.

assigned although they were masked on the ^1H-^{13}C HMQC spectrum by C-3 resonances of sugar units **C**, **D**, **F**, and **G**. Moreover, the complete series of ^1H resonances belonging to sugar unit **B** was also observed.

The ^1H-^{31}P HMQC spectrum of PLM-28 (data not shown) revealed the presence of two ^{31}P resonances connected to the four protons indicated by *arrows* in Fig. 6. Two of these protons were unambiguously assigned to **A**1 and **IN**1 by comparison

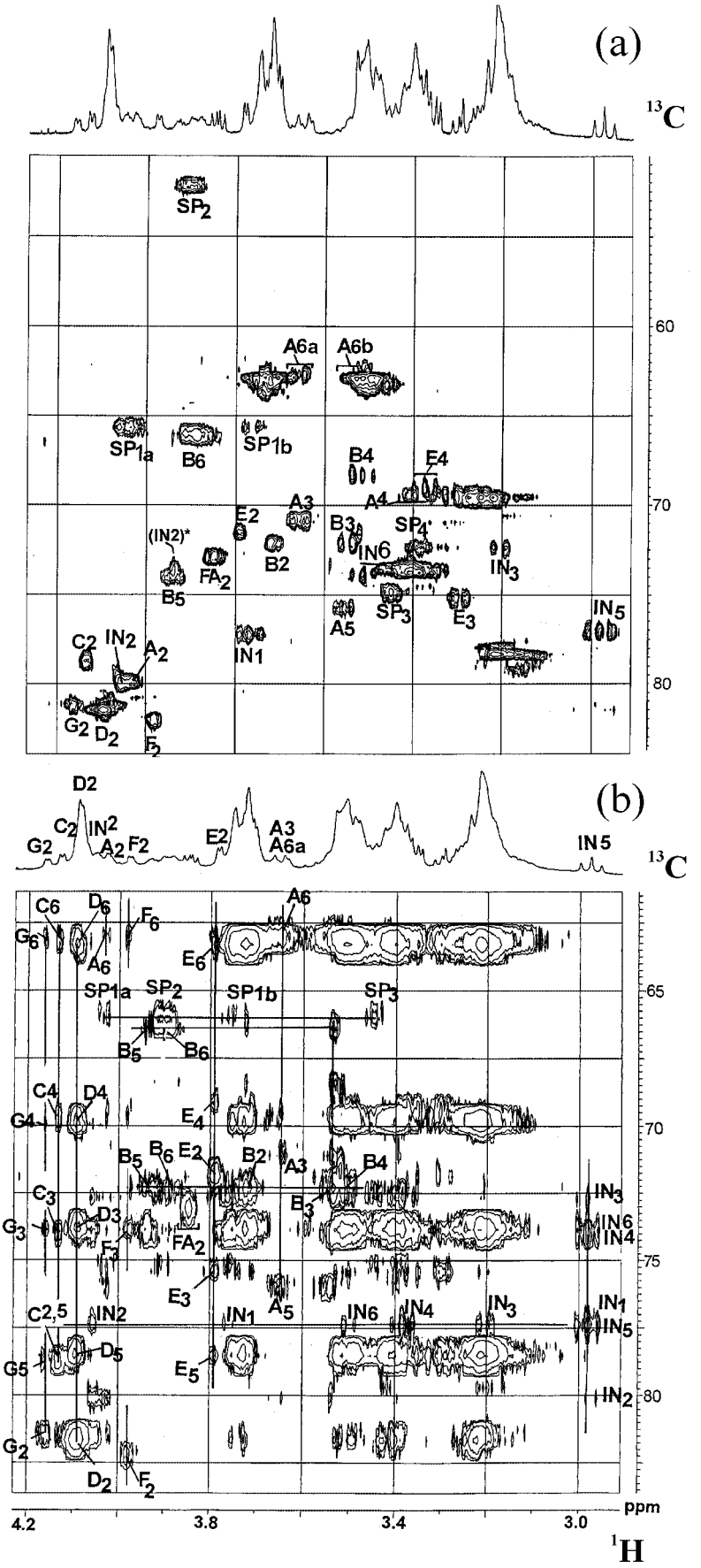

FIG. 5. **^{1}H-^{13}C HMQC (*a*) and HMQC-HOHAHA (*b*) spectra of PLM-28 allowed the assignments of ^{13}C resonances precised in Table III.** Labels **A** to **G**, **IN**, **FA**, and **SP** refer to signals from Man units inositol, fatty acid, and phytosphingosine, respectively. On the HMQC spectrum (*a*), the *x* axis displayed the ^{1}H shifts of protons as previously determined by COSY experiments. Their projection on the *y* axis allowed us to define the corresponding ^{13}C chemical shift. On the HMQC-HOHAHA spectrum (*b*), the ^{1}H/^{13}C correlations were read vertically, *i.e.* from ^{1}H-2 **E** (**E**2) at δ = 3.781, the ^{13}C-6, ^{13}C-4, ^{13}C-2, ^{13}C-3, and ^{13}C-5 signal resonances (noted **E**6, **E**4, **E**2, **E**3, and **E**5) were assigned, respectively. ^{13}C-^{1}H correlations were read horizontally, *i.e.* from ^{13}C-1 signal at δ = 76.85 of inositol **IN**1, the ^{1}H signal resonances **IN5**, **IN**3, **IN**4, **IN**6, and **IN**2 were assigned.

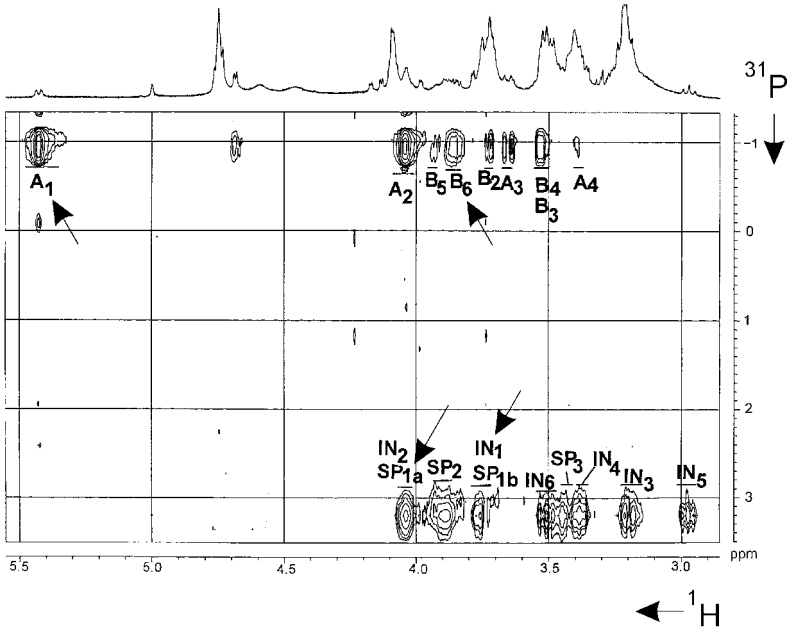

FIG. 6. **^{1}H-^{31}P HMQC-HOHAHA of PLM-37 showed correlations of the ^{31}P signal at $\delta = -0.9$ with mannose units A and B and of the ^{31}P signal at $\delta = 3.2$ with SP and IN.** *Arrows* indicate the position of signals observed on the ^{1}H-^{31}P HMQC spectrum (data not shown).

with the COSY spectrum. The assignment of **SP**1a and **SP**1b ^{1}H resonances was also inferred from this comparison and was in agreement with previous NMR data (7).

The ^{1}H-^{31}P HMQC-HOHAHA spectrum exhibited a complex panel of correlations for the two ^{31}P resonances (Fig. 6). By comparison with the COSY spectra, the **A**2, **A**3, and **B**2 signals could easily be connected with the ^{31}P signal at $\delta = -0.9$. This observation proved the presence of a phosphodiester bridge between the anomeric carbon of sugar unit **A** and one of the carbons of sugar unit **B**. From the ^{1}H-^{13}C HMQC spectrum (Fig. 5*a*) and comparison with the ^{1}H-^{31}P HMQC spectrum, the ^{1}H resonance observed at $\delta = 3.88$, which correlated with a ^{13}C signal at $\delta = 65.85$, could therefore be defined as the H6a-H6b resonance of sugar unit **B**. This assertion was confirmed by the observation of **B**2, **B**3, **B**4, **B**5, and **B**6 horizontal alignment at $\delta = 71.85$ on the ^{1}H-^{13}C HMQC-HOHAHA spectrum (Fig. 5*b*). This observation was consistent with the establishment of the sequence **A**-P-**B**, namely Manα-P-6-Manα. The second line of ^{1}H-^{31}P correlations at $\delta = 3.2$ exhibited the complete **IN** proton spin system as well as the H-1a, H-1b, H-2, and H-3 atom resonances of the phytosphingosine unit (**SP**1a, **SP**1b, **SP**2, and **SP**3). From this observation, the linking structure **IN**-1-P-**SP** was established.

The definitive sequence of PLM was finally achieved through ROESY experiments. The sequences **G**-**F**-**A** and **B**-**IN** were suggested from the interresidual correlations between **G**1-**F**2, **F**1-**A**1, and **B**1-**IN**2 (Fig. 7). Because the ^{1}H-^{31}P HMQC-HOHAHA spectra previously analyzed (Fig. 6) have shown that the two phosphate groups were part of the two sequences **IN**-P-**SP** and **A**-P-6-**B**, the sequence of the linking structure was fully established as α-D-Man*p*-1→P-(O→6)-α-D-Man*p*-(1→2)-**IN**-1-P-(O→1)-**SP**. Concerning the glycan part whose β-1,2-oligomannoside structure was established previously (22), a comparison of the proton and carbon chemical shift values (Table III) provided evidence for the non-reducing terminal position of the β-Man **E** unit. However, for Man units **C** and **D** involved in the repeated sequence of β-1,2-linked mannoses, no more information could be deduced regarding their exact position because of the polydispersity of the molecule.

These results allowed us to define the respective positions of units **A** to **G**, **IN**, **SP**, and the phosphate groups (Fig. 8*a*) and to propose a schematic structure of PLM, which specifies its heterogeneity (Fig. 8*b*)

The split of **IN**2, **IN**3, **IN**6, and **B**1 signals, previously referred to as **IN**2*, **IN**3*, **IN**6*, and **B**1* and observed mainly in PLM-28 (Figs. 4 and 7) appeared to arise from the same molecule, which may correspond to the (M − 2H)/2 molecular-related ion observed on MS spectra at *m/z* 677.94 (Fig. 2*b*). Its deduced mass closely fits the following sequences: Man-α-P-Man-α-Ins-P-Cer or Ins-P-Man-α-Ins-P-Cer (M(IP)2C). We suggest that this structure is most probably $M(IP)_2C$ because: (i) examination of the COSY and HMQC spectra of PLM-28 revealed that β-Man unit **E** was the only one that occurred in the terminal position; (ii) NMR data revealed the absence of a terminal non-reducing α-Man unit; and (iii) the HMQC spectrum of PLM-28 clearly showed that the **IN*** unit was terminal according to its C-2 atom resonance observed at $\delta = 73.5$ (Fig. 5).

DISCUSSION

The poor solubility of glycolipids leading to the formation of micelles is a major limitation to their physicochemical analysis. Therefore, a previous structural study of *C. albicans* PLM has been restricted to its highly soluble glycan part released by saponification (22). This current NMR and MS study has confirmed the two unusual properties of this molecule that were expected from previous immunochemical analyses, *i.e.* the β-anomery of the linkages and the high degrees of polymerization of the oligomannoside chains (22, 28). The presence of two phosphate groups in the molecule was also demonstrated, most probably the first connecting the glycan chain to the lipid moiety and the second presumed to be used to branch a short oligomannoside chain. The presence of this second phosphate group was confirmed by fluorhydric acid hydrolysis that led to a marked modification of the major polymer migration on TLC together with the liberation of a dimannoside or trimannoside (data not shown). The most appropriate method to address the question of the position of the phosphate groups is phosphor/proton NMR analysis. This required: i) the purification of large quantities of PLM (>5 mg), ii) the analysis of the whole molecule since saponification was shown to affect the environment of at least one phosphate group and to induce an additive heterogeneity of the mass spectra (22), and iii) high solubility of the whole molecule in a solvent system. These problems were overcome by improving the step-by-step purification procedure and by using as the solvent for NMR studies dimethyl sulfoxide, which allowed a better solubility of PLM than H_2O.

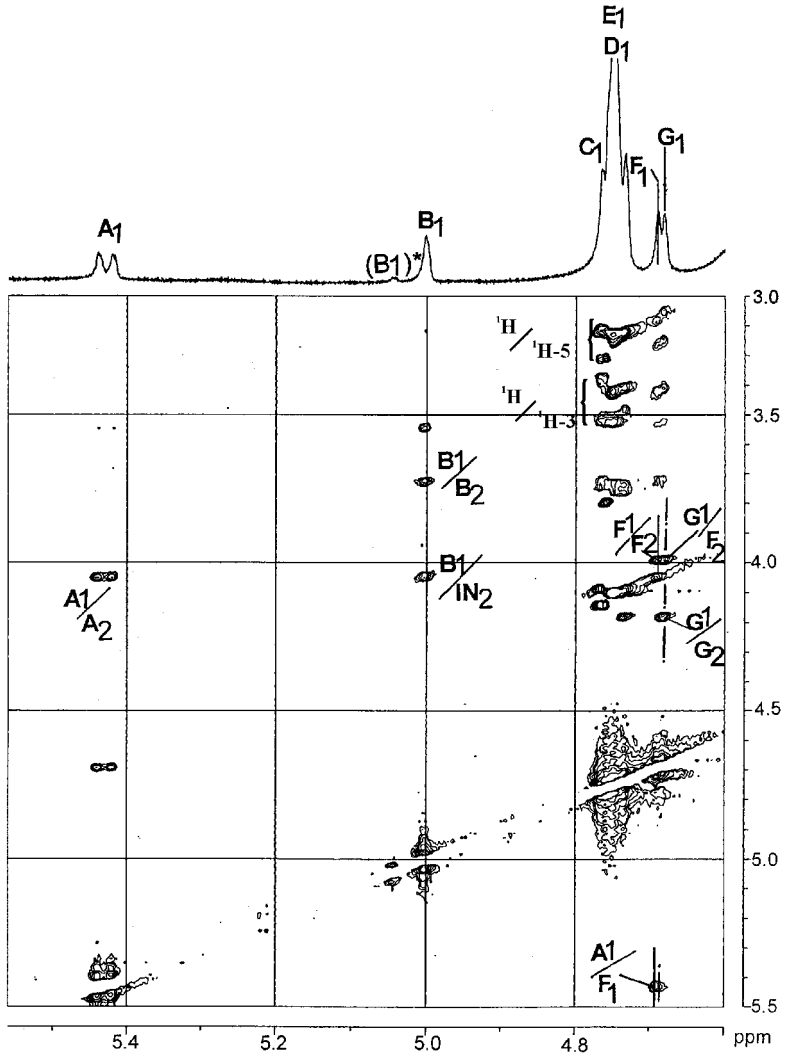

FIG. 7. **ROESY spectrum of PLM-37.** α-Man units **A** and **B** were characterized by H-1/H-2 intraresidual NOE contacts, whereas β-Man units **C** to **G** showed intense H-1/H-3, and H-5 intraresidual connectivities. Interresidual correlations between **A** to **F** and **B-IN** are also observed.

(a)

E **C,D** **G** **F** **A** **B** **IN** **SP** **FA**

β-D-Man*p*-(1→2)-[β-D-Man*p*-(1→2)]$_n$-β-D-Man*p*-(1→2)-β-D-Man*p*-(1→2)-α-D-Man*p*-1→P-(O→6)-α-D-Man*p*-(1→2)-Ins-1-P-(O→1)-PHS-FA

(b)

[β-D-Man*p*-(1→2)]-α-D-Man*p*-1→P-(O→6)-α-D-Man*p*-(1→2)-Ins-1-P-(O→1)-Cer

1 to 18

FIG. 8. **Schematic structure of PLM of *C. albicans* strain VW32, serotype A.** *a*, detailed structure showing the position in the molecule of the components that displayed nuclear magnetic resonance signals **A** to **G**, **IN**, **SP**, and **FA**. *b*, general structure of PLM pointing out the heterogeneity of its glycan moiety. The ceramide moiety (*Cer*) also heterogeneous is mainly composed of rC_{18} PHS-OH rC_{24} FA for PLM at 28 °C or rC_{20} PHS-OH rC_{24} FA for PLM at 37 °C.

Methanolysis of PLM revealed the presence of rC_{18} or rC_{20} PHS and rC_{24}, rC_{25}, or rC_{26} hydroxylated fatty acids in addition to mannoses and inositol. These results showed that PLM is related to the family of IPC, MIPC, and $M(IP)_2C$ previously observed in *C. albican*s (21). Nevertheless, the electron impact spectra of methanolysis products newly evidenced predominant branched aliphatic chains in both the long chain bases and fatty acids of the ceramide moiety.

As shown previously, the glycan chain was the major source of heterogeneity of the molecule because electrospray mass spectrometry revealed 3–20 mannose units/molecule, the majority of PLM molecules presenting >11 mannose units. Such heterogeneity could be constitutive or may result from the different steps of biosynthesis. The first hypothesis is more coherent with Western blot analysis of cell wall extracts of *C. albicans* that are supposed to contain mature PLM, which nevertheless revealed heterogeneity of the molecule.[2] However, mass spectrometry together with analysis of methanolysis products also demonstrated the heterogeneity of the ceramide moiety. This was based mainly on the presence of both rC_{18} and rC_{20} PHS and concerned all PLM molecules, irrespective of the degree of polymerization of their glycan part. This finding suggests that the constant heterogeneity of the ceramide moiety results from the first steps of synthesis rather than from remodeling of the mature glycolipids as described for *S. cerevisiae* GPI anchors (15). However, the major difference observed in rC_{18} PHS and rC_{20} PHS ratios by both methods was related to growth temperature, the rC_{20} PHS becoming predominant when temperature shifted from 28 to 37 °C. Such an increase in

[2] P.-A. Trinel, E. Maes, J.-P. Zanetta, F. Delplace, B. Coddeville, T. Jouault, G. Strecker, and D. Poulain, unpublished data.

the C_{20}/C_{18} PHS ratio has also been reported for *S. cerevisiae* during heat shock. It was transient for free PHS (15 min) but more stable for PHS found in phytoceramides (at least 1 h) (32) and was proposed to act as a key signaling event in the heat stress response including the induction of trehalose accumulation (32), a cellular thermoprotectant (33). Therefore, it seems that *C. albicans* and *S. cerevisiae* respond similarly to temperature by increasing C_{20} PHS. However, this increase is continuous, and rC_{20}/rC_{18} PHS ratios are more important in *C. albicans* for which the consequences of this shift on both yeast cell metabolism and host-parasite relationships remain to be determined.

Similar modifications linked to growth temperature were also observed in a molecule associated with our PLM preparations with the characteristics of $M(IP)_2C$, the main sphingolipid of plasma membranes (3). This was deduced from MS analysis, which displayed the expected masses related to variability of the ceramide moiety similar to that of PLM, whereas NMR studies revealed additional **IN**2*, **IN**3*, and **IN**6* signals arising from unsubstituted inositol. The presence of this structurally related molecule was not surprising because our purification procedure was designed to address to the whole PLM family, which encompasses a number of molecules that diverge according to their amphipathic character. Among these, poorly glycosylated PLMs have physicochemical properties closely related to $M(IP)_2C$. We may also expect in the peaks allocated to $M(IP)_2C$ a minor interference of Man-P-Man-IPCs that display the same masses and correspond to the first biosynthesis step specific for PLM

However, because of the selectivity of the NMR signals, the presence of $M(IP)_2C$ did not change the interpretation of our results and allowed us to determine the general structure of PLM, particularly the position of the two phosphate groups. As suggested previously, the first phosphate group links the inositol to the PHS of the lipid moiety. The second group, formerly thought to be used for branching a short lateral oligomannoside chain, appears to be a component of the spacer that links the β-1,2-oligomannoside chain to the lipid anchor. The structure of this spacer (-Man-P-Man-Ins-P-), although closely related to the polar group of $M(IP)_2C$, -Ins-P-Man-Ins-P-, has never been described for a glycosphingolipid and appears to be more complex than those of other fungal glycoinositol sphingolipids (8) including those characterized in higher mushrooms (7). Thus, the synthesis of PLM appears to follow the biosynthetic pathway of major membrane sphingolipids from fungi, IPC, MIPC, and $M(IP)_2C$ from which it should diverge at the MIPC step by further addition of mannosyl phosphate instead of inositol phosphate. In contrast to the addition of inositol phosphate that leads to $M(IP)_2C$, an end-biosynthesis product that is not mannosylated further, the addition of mannosyl phosphate is followed by stepwise β-1,2-mannosylations, leading to unusual linear chains containing up to 19 Man units. These chain lengths are indeed unique when compared with the glycan part of other fungal glycoinositol phosphosphingolipids that never exceed six sugar units (7, 8). They are also longer than those of β-1,2-oligomannosides from *C. albicans* mannan, which never exceed 14 Man units (34). These chains confer on PLM marked hydrophilic properties, which differentiate this molecule from IPC, MIPC, and $M(IP)_2C$ whose hydrophobic characteristics are coherent with their membrane location. These hydrophilic properties explain why PLM may be released from the cell wall and is ultimately shed from the *C. albicans* cell surface. In the presence of macrophages, PLM is used by *C. albicans* as a vector for β-1,2-oligomannosides, and shedding of this molecule induces intense signal transduction pathways (27). From a pathophysiological point of view, PLM appears to be a new member of the inositol containing glycolipids described in microbial pathogens, which favor their survival in the host and/or modify its immune response (35–38).

Elucidation of the complete structure of PLM (Fig. 8*b*) was a necessary step to determine its biosynthetic pathway and to specify its role in *C. albicans*, particularly its role in yeast-yeast or yeast-host cells interactions (related to hydrophobicity) (39). This structure also provides the basis for the identification of yeast genes involved in PLM biosynthetic pathways with the ultimate aim of constructing *C. albicans* PLM-deficient mutants (12). Such studies are currently underway and will help to determine the importance of PLM to the fungal cell and as a virulence factor.

Specific inhibition of mannan β-mannosylation related to growth of *C. albicans* at acidic pH (40) or high temperature (41, 42) has previously been demonstrated. However, neither conditions had any affect on PLM β-1,2-mannosylation. Interestingly, a comparison of mannan and PLM structures now shows that β-mannosylation of both molecules starts from the same -Manα-P-6-Manα- group. Whether the nature of the acceptor molecule for β-1,2-oligomannosides is regulated by transcription pathways will be an interesting question to address.

In conclusion, this study shows that the prominent opportunistic fungal pathogen *C. albicans* uses the biosynthetic pathway of membrane sphingolipids to express an unusual linear mannose polymer of β-1,2-linked mannose on its surface. As β-1,2-oligomannosides are known to have an important role as adhesins, induce cytokine production, and generate protective antibodies, it can be anticipated that this alternative mode of presentation to host cells may have some significance in terms of pathogenesis.

Acknowledgments—We thank Annick Masset for technical assistance and Dr. Valerie Hopwood for helpful suggestions on this paper.

REFERENCES

1. Hakomori, S. (1996) *Cancer Res.* **56,** 5309–5318
2. Schnaar, R. L., Mahoney, J. A., Swank-Hill, P., Tiemeyer, M., and Needham, L. K. (1994) *Prog. Brain Res.* **101,** 185–197
3. Patton, J. L., and Lester, R. L. (1991) *J. Bacteriol.* **173,** 301–308
4. Hannun, Y. A. (1996) *Science* **274,** 1855–1859
5. Ballou, L. R., Laulederkind, S. J., Rosloniec, E. F., and Raghow, R. (1996) *Biochim. Biophys. Acta* **1301,** 273–287
6. Merrill, A. H., and Sweeley, C. C. (1996) in *Biochemistry of Lipids, Lipoproteins and Membranes* (Vance, D. E. and Vance., J. E., eds), pp. 309–339, Elsevier Science Publishers B.V., Amsterdam
7. Jennemann, R., Geyer, R., Sandhoff, R., Gschwind, R. M., Levery, S. B., Grone, H. J., and Wiegandt, H. (2001) *Eur. J. Biochem.* **268,** 1190–1205
8. Dickson, R. C., and Lester, R. L. (1999) *Biochim. Biophys. Acta* **1426,** 347–357
9. Dickson, R. C. (1998) *Annu. Rev. Biochem.* **67,** 27–48
10. Zhong, W., Jeffries, M. W., and Georgopapadakou, N. H. (2000) *Antimicrob. Agents Chemother.* **44,** 651–653
11. Mandala, S. M., Thornton, R. A., Rosenbach, M., Milligan, J., Garcia-Calvo, M., Bull, H. G., and Kurtz, M. B. (1997) *J. Biol. Chem.* **272,** 32709–32714
12. Dickson, R. C., and Lester, R. L. (1999) *Biochim. Biophys. Acta* **1438,** 305–321
13. Chung, N., Mao, C., Heitman, J., Hannun, Y. A., and Obeid, L. M. (2001) *J. Biol. Chem.* **276,** 35614–35621
14. Patton, J. L., Srinivasan, B., Dickson, R. C., and Lester, R. L. (1992) *J. Bacteriol.* **174,** 7180–7184
15. Reggiori, F., Canivenc-Gansel, E., and Conzelmann, A. (1997) *EMBO J.* **16,** 3506–3518
16. Zanolari, B., Friant, S., Funato, K., Sutterlin, C., Stevenson, B. J., and Riezman, H. (2000) *EMBO J.* **19,** 2824–2833
17. Zhao, C., Beeler, T., and Dunn, T. (1994) *J. Biol. Chem.* **269,** 21480–21488
18. Beck-Sague, C., and Jarvis, W. R. (1993) *J. Infect. Dis.* **167,** 1247–1251
19. Pfaller, M. A., Jones, R. N., Messer, S. A., Edmond, M. B., and Wenzel, R. P. (1998) *Diagn. Microbiol. Infect. Dis.* **31,** 327–332
20. Matsubara, T., Hayashi, A., Banno, Y., Morita, T., and Nozawa, Y. (1987) *Chem. Phys. Lipids* **43,** 1–12
21. Wells, G. B., Dickson, R. C., and Lester, R. L. (1996) *J. Bacteriol.* **178,** 6223–6226
22. Trinel, P. A., Plancke, Y., Gerold, P., Jouault, T., Delplace, F., Schwarz, R. T., Strecker, G., and Poulain, D. (1999) *J. Biol. Chem.* **274,** 30520–30526
23. Li, R. K., and Cutler, J. E. (1993) *J. Biol. Chem.* **268,** 18293–18299
24. Fradin, C., Poulain, D., and Jouault, T. (2000) *Infect. Immun.* **68,** 4391–4398
25. De Bernardis, F., Boccanera, M., Adriani, D., Spreghini, E., Santoni, G., and Cassone, A. (1997) *Infect. Immun.* **65,** 3399–3405
26. Han, Y., Kanbe, T., Cherniak, R., and Cutler, J. E. (1997) *Infect. Immun.* **65,** 4100–4107
27. Jouault, T., Fradin, C., Trinel, P. A., Bernigaud, A., and Poulain, D. (1998)

J. Infect. Dis. **178,** 792–802
28. Trinel, P. A., Borg-von-Zepelin, M., Lepage, G., Jouault, T., Mackenzie, D., and Poulain, D. (1993) *Infect. Immun.* **61,** 4398–4405
29. Zanetta, J. P., Timmerman, P., and Leroy, Y. (1999) *Glycobiology* **9,** 255–266
30. Pons, A., Popa, J., Portoukalian, J., Bodennec, J., Ardail, D., Kol, O., Martin-Martin, M. J., Hueso, P., Timmerman, P., Leroy, Y., and Zanetta, J. P. (2000) *Anal. Biochem.* **284,** 201–216
31. Pons, A., Timmerman, P., Leroy, Y., and Zanetta, J. P. (2002) *Lipid Res.* **43,** 794–804
32. Dickson, R. C., Nagiec, E. E., Skrzypek, M., Tillman, P., Wells, G. B., and Lester, R. L. (1997) *J. Biol. Chem.* **272,** 30196–30200
33. De Virgilio, C., Hottiger, T., Dominguez, J., Boller, T., and Wiemken, A. (1994) *Eur. J. Biochem.* **219,** 179–186
34. Trinel, P. A., Lepage, G., Jouault, T., Strecker, G., and Poulain, D. (1997) *FEBS Lett.* **416,** 203–206
35. Barnes, P. F., Chatterjee, D., Abrams, J. S., Lu, S., Wang, E., Yamamura, M., Brennan, P. J., and Modlin, R. L. (1992) *J. Immunol.* **149,** 541–547
36. Dahl, K. E., Shiratsuchi, H., Hamilton, B. D., Ellner, J. J., and Toossi, Z. (1996) *Infect. Immun.* **64,** 399–405
37. Schofield, L., and Tachado, S. D. (1996) *Immunol. Cell Biol.* **74,** 555–563
38. Yoshida, A., and Koide, Y. (1997) *Infect. Immun.* **65,** 1953–1955
39. Masuoka, J., and Hazen, K. C. (1999) *Glycobiology* **9,** 1281–1286
40. Kobayashi, H., Giummelly, P., Takahashi, S., Ishida, M., Sato, J., Takaku, M., Nishidate, Y., Shibata, N., Okawa, Y., and Suzuki, S. (1991) *Biochem. Biophys. Res. Commun.* **175,** 1003–1009
41. Okawa, Y., Takahata, T., Kawamata, M., Miyauchi, M., Shibata, N., Suzuki, A., Kobayashi, H., and Suzuki, S. (1994) *FEBS Lett.* **345,** 167–171
42. Okawa, Y., Goto, K., Nemoto, S., Akashi, M., Sugawara, C., Hanzawa, M., Kawamata, M., Takahata, T., Shibata, N., Kobayashi, H., and Suzuki, S. (1996) *Clin Diagn. Lab. Immunol.* **3,** 331–336